



NRC Publications Archive Archives des publications du CNRC

In-line compounding of direct long fibre thermoplastics: injection versus compression moulding

McLeod, M.; Baril, É.; Hétu, J.-F.; Deaville, T.; Bureau, M. N.

This publication could be one of several versions: author's original, accepted manuscript or the publisher's version. /
La version de cette publication peut être l'une des suivantes : la version prépublication de l'auteur, la version acceptée du manuscrit ou la version de l'éditeur.

Publisher's version / Version de l'éditeur:

Design, Manufacturing and Applications of Composites: Proceedings of the Eighth Joint Canada-Japan Workshop on Composites, 2010-07-26

NRC Publications Record / Notice d'Archives des publications de CNRC:

<https://nrc-publications.canada.ca/eng/view/object/?id=5e728920-cb11-49f9-9be7-da302c19ce42>
<https://publications-cnrc.canada.ca/fra/voir/objet/?id=5e728920-cb11-49f9-9be7-da302c19ce42>

Access and use of this website and the material on it are subject to the Terms and Conditions set forth at

<https://nrc-publications.canada.ca/eng/copyright>

READ THESE TERMS AND CONDITIONS CAREFULLY BEFORE USING THIS WEBSITE.

L'accès à ce site Web et l'utilisation de son contenu sont assujettis aux conditions présentées dans le site

<https://publications-cnrc.canada.ca/fra/droits>

LISEZ CES CONDITIONS ATTENTIVEMENT AVANT D'UTILISER CE SITE WEB.

Questions? Contact the NRC Publications Archive team at

PublicationsArchive-ArchivesPublications@nrc-cnrc.gc.ca. If you wish to email the authors directly, please see the first page of the publication for their contact information.

Vous avez des questions? Nous pouvons vous aider. Pour communiquer directement avec un auteur, consultez la première page de la revue dans laquelle son article a été publié afin de trouver ses coordonnées. Si vous n'arrivez pas à les repérer, communiquez avec nous à PublicationsArchive-ArchivesPublications@nrc-cnrc.gc.ca.



In-line compounding of direct long fibre thermoplastics: injection versus compression moulding

M. McLeod¹, É. Baril¹, J.-F. Héту¹, T. Deaville² and M. N. Bureau¹

¹ Industrial Materials Institute, National Research Council Canada, 75 de Mortagne, Boucherville (Québec) Canada, J4B 6Y4

² Magna Exteriors and Interiors Corp., 50 Casmir Court, Concord (Ontario) Canada, L4K 4J5

ABSTRACT

Long fibre thermoplastics (LFT) based on polypropylene/glass fibre (PP/GF) composites has become one of the most widely used plastics in semi-structural and structural automotive applications in both aesthetic and non-aesthetic parts. LFT are commercially available in pre-compounded pellets for injection moulding and are developed with specific properties for targeted functions. In a rationalizing effort to reduce costs, heat histories, and create in-house flexibility of material blending in-line compounding (ILC) of base materials including resin, additives (heat stabilizers, colors, coupling agents, etc.), and glass roving reinforcements for direct moulding of LFT parts (D-LFT) has been developed in the last 10 years. Two major versions of D-LFT technology currently exist on the market, both relying on twin-screw extrusion (one-stage or two-stage) for ILC, one utilizing compression moulding and the other injection moulding. While these two technologies share several similarities, they also present significantly different features in terms of fibre length, orientation and mechanical properties for example, related to their respective processing conditions. The objective of this paper is to address some of them.

A Dieffenbacher LFT Direct system, using the compression moulding process, and a Krauss-Maffei Injection Moulding Compounder (IMC), using the injection moulding process, were used to mould similar test parts that have a significant level of complexity in their geometry. Samples were taken from the parts and from machine purges for a comparison of the respective fibre distribution patterns of the two moulding technologies using micro focus X-ray computed tomography. A characterization of their fibre length distribution was also performed on these samples from pyrolysis and image analysis. Resulting mechanical properties were then added to the comparison matrix to provide a comprehensive picture of the two moulding technologies.

INTRODUCTION

Despite their inherent advantages in terms of manufacturing costs, weight-effectiveness, structural/impact properties and recyclability [1], continuous or long fibre reinforced thermoplastic composites have not found applications in the North American automotive industry to their full potential. The key challenge associated with their adoption by the industry remains high-throughput production, *i.e.* very large quantities (>500,000 parts) at an affordable cost, and limitations in their thermal/dimensional stability during the surface finish operations for aesthetic parts. Pre-compounded LFT materials (glass or carbon fibres PP, PA6, PA66, etc.) in the form of pellets are currently available and while they do provide answers to functional requirements like heat deflection temperature (HDT), stiffness and strength, their cost and fracture-related properties (flat sheet impact, Izod/Charpy, etc.) have limited their penetration in the automotive marketplace. The automotive industry has identified Direct-Long Fibre Thermoplastic (D-LFT) technology as one of the enabling manufacturing system through which thermoplastic composites will be widely adopted by the automotive industry for structural and aesthetic (body panels) applications [2].

The D-LFT technology is a combined continuous in-line compounding (ILC) process using a thermoplastic matrix, additives and fibre reinforcements combined with either compression or injection moulding. State-of-the-art D-LFT technology currently in use with polypropylene-long glass fibre composites has been shown to be the system of choice for many automotive applications when it comes to reducing costs and saving weight for improved fuel economy [3]. D-LFT is already in production on a variety of semi-structural parts, including non-appearance parts such as under body shields, radiator supports, spare tire tubs, etc., as well as grained non class A appearance parts such as running boards [4]. New automotive structural parts based on this D-LFT technology are currently being contemplated and even produced in some cases by North American auto makers and their suppliers to take advantage of this weight reduction and cost savings.

The struggle for manufacturers has been the decision between utilizing a compression or injection system along with the ILC system to cost effectively produce parts with the required properties. Significant side by side studies of compression and injection parts have not typically taken place in the industry due to the new nature of the technology in North America, the competitive nature of this comparison and because of the costs associated with accessing the high capital investment equipment to perform this comparison. To this aim, the goal of the present study is to obtain qualitative and quantitative comparison of the similar components produced by ILC/compression and ILC/injection, by characterizing their respective fibre distribution patterns and fibre length distribution. These resulting fibre characteristics were then compared at different stages and between the two moulding technologies. Resulting mechanical properties were also obtained to provide a comprehensive picture of the two moulding technologies.

MATERIALS AND METHODS

Two D-LFT systems were used to obtain sample purgings and to mould the test parts. The first system was a Dieffenbacher LFT Direct system, using the compression moulding process (LFT-D-ILC Type ZSG Mixing Extruder and a 2000 ton compression press). The second system was a Krauss Maffei IMC Injection Moulding Compounder, using the injection moulding process (1000 ton MX Series with ZE75 twin screw extruder). The two systems will be referred to as DLFT-Compression and DLFT-Injection respectively. The materials used were a standard PP/GF composite made up of a generic homopolymer polypropylene from Dow, masterbatches supplied by Addcomp and Dow and a general purpose polyolefin glass fibre rovings supplied by Owens Corning and Jushi. The test parts used for the study are structural automotive parts as would typically be found in applications both in North America and Europe. The part has many structural features such as thicker wall stock (+5 mm), many ribs and mounting surfaces. The parts typically weighted 1.1 kg. The same mould was used for both DLFT systems (with slight modification at the nozzle for DLFT-Injection). Nominal GF content was 40% by weight. The DLFT-Compression and DLFT-Injection processes were not fully optimized for this study.

The moulded parts were analysed with an X-Tek HMXST 225 X-ray microtomography (MicroCT) system (Metris, Tring, UK). The system is equipped with a 225 kV microfocus X-ray tube producing a cone beam that is detected using a PE 1621 AN amorphous silicon 409.6X409.6 mm flat panel sensor coupled with CsI scintillator screen (PerkinElmer Optoelectronics, Fremont, CA). The 3D cone beam reconstruction, by Feldkamp-Davis-Kress (FDK) algorithm, was done with X-Tek CT Pro software. Typical scan parameters were 90kV and 0.55 mA with the flat panel acquisition time was set to 1 s and 8 frames average was used for each projection. X-ray images were taken every 0.1462° for a rotation angle of 360° which results in 2463 images. The highest spatial resolution of the reconstructed 3D volume was 32 µm. For the largest samples, the resolution was reduced to 75 µm for dataset handling purpose.

For both DLFT systems, samples were taken just prior to moulding, i.e., at the injection nozzle of the DLFT-Injection system and the exit of the extruder for the DLFT-Compression system (log). Samples were also cut from both types of moulded parts at similar places for detailed microtomography and fibre length measurements. Fibre length measurements were made from pyrolyzed samples (500°C, 3 hours) using an optical low magnification microscope (Zeiss, 3-10X). Care was taken to make sure samples came from the same location in both parts. Glass fibre lengths were measured using an image analyser. Fibre length distributions were then obtain from individual fibre length measurements at a low magnification chosen to ensure fibres with length between 2-4 mm and +50 mm could be measured. The minimum count of fibres was 320 to 400 for the samples with the longest fibres and more than 500 for those with shorter fibres. From the fibre length distribution obtained, the number-average and weight-average fibre lengths \bar{l}_n and \bar{l}_w were calculated according to Equations 1 and 2. A fibre length distribution (FLD) index was then extracted from the ratio of weight to number-average fibre length. A FLD close to one indicates a near monodispersed FL distribution, while

one diverging above one is indicative of a polydispersed distribution (large and small FL populations).

$$\bar{l}_n = \frac{\sum n_i \cdot l_i}{\sum n_i} \quad (1)$$

$$\bar{l}_w = \frac{\sum n_i^4 \cdot l_i^4}{\sum n_i^3 \cdot l_i^3} \quad (2)$$

Samples were also taken from both types of moulded parts at similar locations for mechanical characterization. The first series of samples were taken from a mounting flange at the bottom of the moulded parts (away from the central injection point for the DLFT-Injection parts) and had a thickness of 3.15 to 4.33 mm depending on sample location. The second series of samples were taken from the central portion of the part in a thick wall section and had a thickness of 8.0 mm. Since these latter samples have a trapezoidal section, they had to be resurfaced. Flexural testing was performed using an electro-mechanical universal tester (INSTRON 55R1123) according to the general requirements of ASTM D790M for three-point bending tests. However, since the specimens did not have the same thickness from one location to the other, the support span distance and crosshead speed was adjusted for each test to satisfy the requirements for a span to thickness ratio of 16:1 and a strain rate of 0.01 s^{-1} . The flexural modulus, flexural yield stress and flexural yield strain was calculated according to ASTM D790 respectively for the slope, the maximum load and the deflection at maximum load on the load-deflection curves.

RESULTS AND DISCUSSION

Fibre Distribution Pattern

The microCT slices of the complete section of molten LFT material just prior to introduction into the mould either by extruded log transfer for ILC-Compression or injection nozzle purge for ILC-Injection are shown in Figure 1. The microCT slices of the extruded log (Fig. 1a) showed the presence of an external envelop, formed by a high density of GF rovings, virtually wrapping the extruded log. They also showed the formation of a typical double helix structure that can be related to the co-rotating twin screws utilised during ILC for this process. A region between these two swirls appeared to contain a high density of GF rovings. The microCT 3D reconstruction resolution being $75 \text{ }\mu\text{m}$, the darker and brighter zones within the log reveal the formation of GF-rich zones and GF-depleted zones within the log, with a generally uneven GF distribution within the extruded log. The overall GF content remained a nominal 40% throughout the purge samples.

By contrast, the microCT slices of the injection nozzle purge (Fig. 1b), obtained in the same MicroCT conditions as for the microCT slices of the extruded log, did not reveal the presence of cord-like structures indicative of GF-rich zones possibly associated with GF bundles or rovings. Therefore, it appears that GF were well distributed within the injection nozzle purge for ILC-injection, or at least that GF rovings or bundles were opened and individual GF separated by less than the microCT spatial

resolution of 75 μm . From the microCT slices shown, it is not possible to obtain information about GF orientation within the injection nozzle due to the fact that GF are uniformly distributed and that GF diameter (approx. 20 μm) is significantly smaller than spatial resolution of the 3D reconstruction (75 μm).

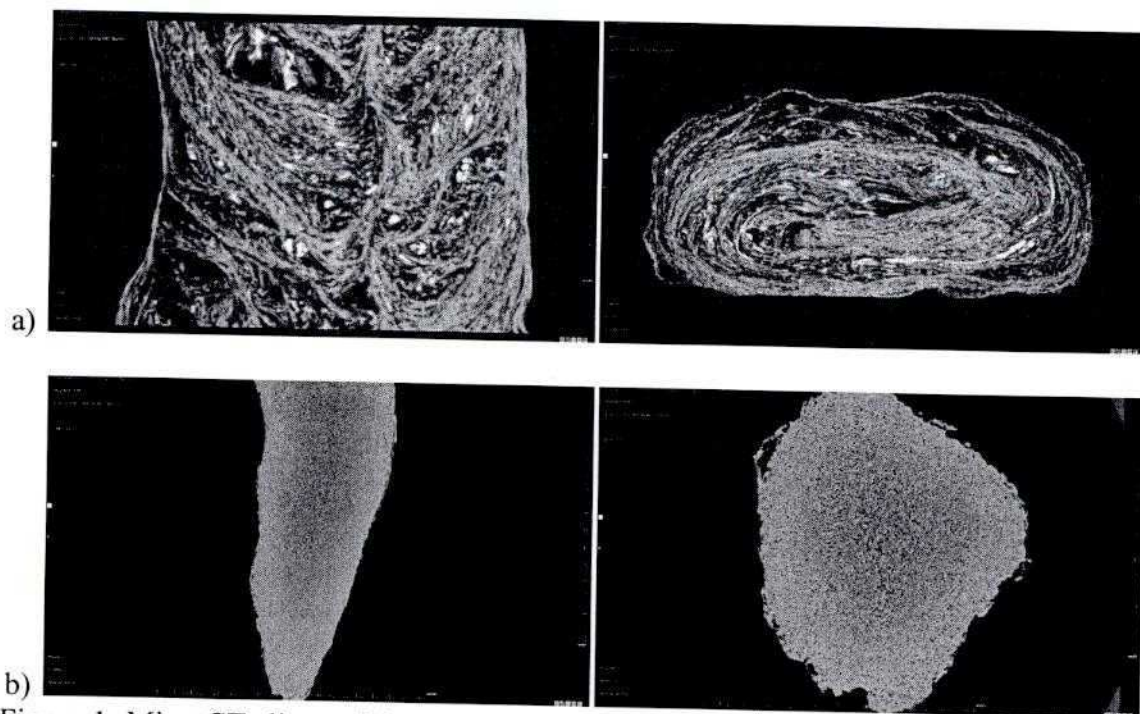


Figure 1. MicroCT slices of the ILC-Compression (a) and ILC-Injection (b) just prior to introduction into the mould either by log (log width and height \approx 125 mm and 75 mm) transfer for ILC-Compression or injection nozzle purge for ILC-Injection. The spatial resolution of these 3D reconstructions was 75 μm . Brighter zones indicate higher density in GF, while darker zones indicate lower GF presence (individual fibres may be present). Uniform brightness areas indicate zone with uniform GF content.

The X-ray radiographs of both types of moulded parts are shown in Figure 2. They reveal very different GF distributions for both types of moulded parts. For ILC-Compression, GF patterns are visible at the bottom section of the moulded part. They show no specific orientation within the bottom plane, as expected from the compression of the extruded molten log. In Figure 2 again, GF-rich zones and GF-depleted zones, indicating a somewhat uneven GF distribution within the moulded part, at least in its bottom section. On the contrary, ILC-Injection shows very few GF patterns, which indicates a more even distribution locally of the GF and matrix. As in the case of the injection nozzle microCT slices, the fact that individual fibers are not visible is simply the result of the radiographs resolution adjusted to obtain a complete view of the moulded part. Since the X-ray radiographic imaging conditions were the same for both observations, it is correct to conclude that GF are better distributed within the ILC-Injection moulded part than ILC-Compression moulded part. For the latter observations,

however, it is not possible to comment of individual GF length distribution. For both processes, the overall GF content remained a nominal 40% throughout the part samples.

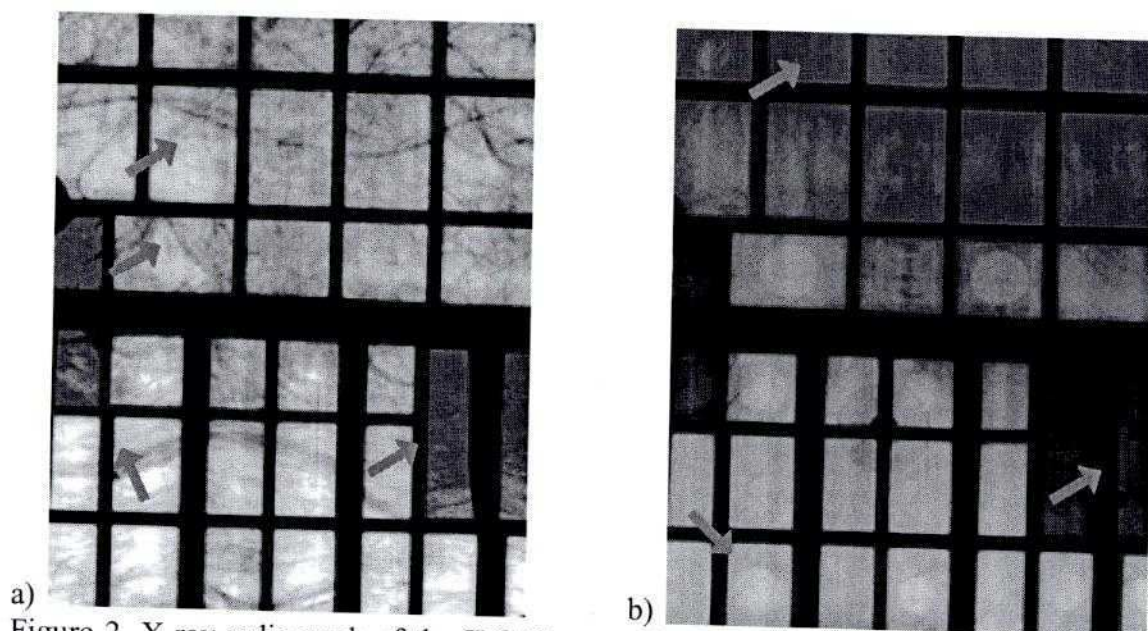


Figure 2. X-ray radiograph of the ILC-Compression (a) and ILC-Injection (b) moulded part showing thicker wallstocks (+5 mm), ribs and mounting surfaces. Fibre pattern (blue arrows) can be observed at several locations in ILC-Compression part but at very few locations in ILC-Injection part.

MicroCT observations of several individual rib sections were performed to obtain a more complete understanding of the GF patterns within the part. An example of these observations is shown in Figure 3. Individual rovings can be observed in both sections but GF distribution appears generally uniform in the ILC-Injection case. ILC-Compression section shows GF-rich and GF-depleted zones but to a far lesser extent than expected from observations on Figure 2. Note the presence of a GF-rich site in the right-hand side section of the microCT slice of the ILC-Injection, while the remaining portion of the section shows uniform GF distribution. This point of the part is opposite to the injection point (gate) which is not visible on this orientation. This observation is surprising since individual GF bundles or GF-rich zones were not observed within the injection nozzle. This suggests either that the injection feedstock (nozzle sample) is not representative of the material injected in the component when the mould is closed and the additional; or that injection forces are present as opposed to when the purge is made into open atmosphere or the flow paths in the ribs of the component close to the injection point is forcing some kind of fibre alignment and segregation which is showing up in the moulded part. Unfortunately, the spatial resolution required to see a significant portion of the component does not resolve individual fibre and, therefore, no conclusion can be drawn about fibre orientation and the distribution of individual GF length. Fibre burn off sections must therefore be analysed to provide this information.

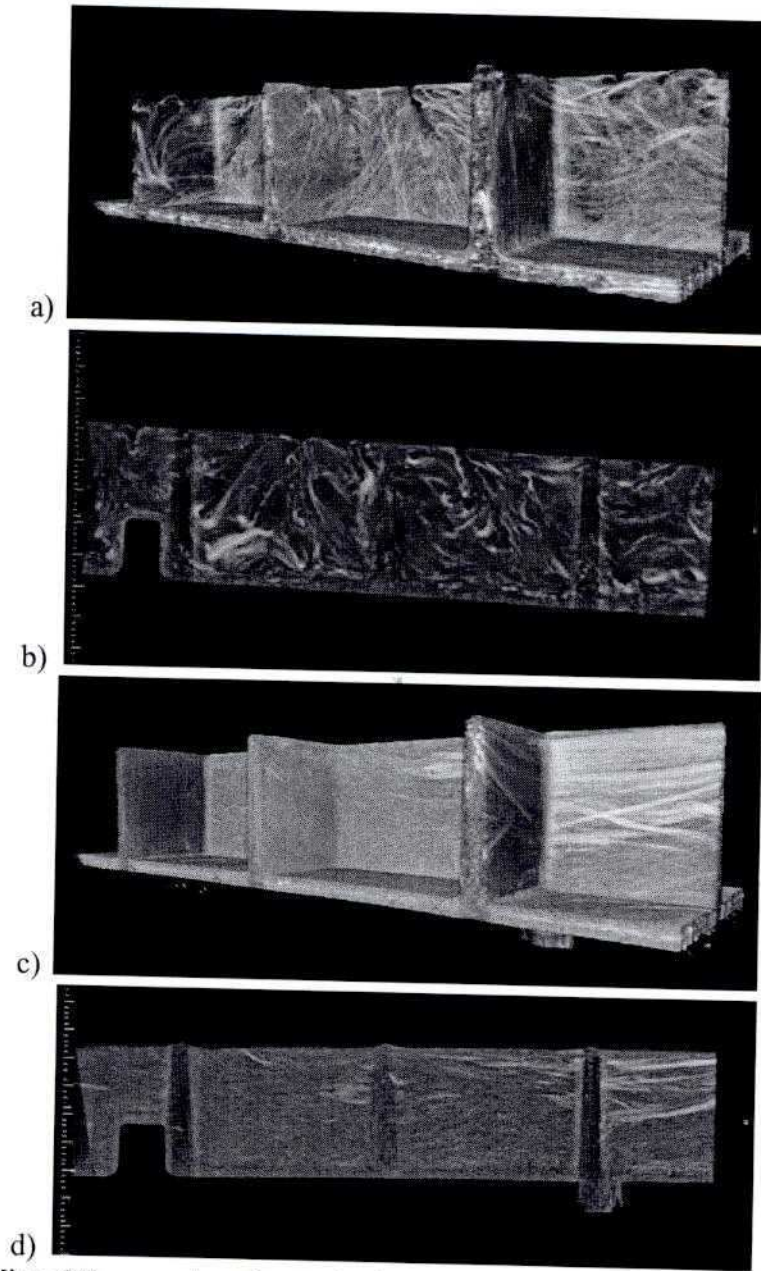


Figure 3. 3D MicroCT reconstruction and microCT slice along the long vertical rib of the ILC-Compression (a and b) and ILC-Injection (c and d) moulded part at a cross rib section taken from the bottom zone of the part. The spatial resolution of these 3D reconstructions was 32 μm .

Fibre Length Distribution

Fibre burn off sections were taken from the ILC-Compression and ILC-Injection moulded parts. Cumulative FL distributions were obtained from the log/injection nozzle purge and from a wall section in the moulded parts. The number-average and weight-average fibre lengths \bar{l}_n and \bar{l}_w , and related fibre length distribution (FLD) obtained at

these two locations are reported in Table I, as well as for a rib location elsewhere in the moulded parts for which the fibre length distribution is not shown (for concision). As expected from previous studies as well as microCT observations shown herein, FL results indicate that the extruded log from ILC-Compression contained considerably longer fibres than the injection nozzle purge from ILC-Injection. Typically, both the number-average and weight-average FL from the extruded log were more than twice as much as those from the injection nozzle purge. These expected results can potentially be attributed to a number of factors rooted in the different configurations of the ILC systems. First the two-stage compounding of the ILC-Compression where GF are introduced in the second compounding stage and as a result are subjected to less shear history. Next there is the direct extrusion of the log in line from the second compounding stage of the ILC-Compression system as opposed to the use of an accumulator and a shooting pot both of which are at right angles and 180° opposed respectively, subjecting the material in the ILC-Injection system to additional shear. And finally the ILC-Compression system preconditions the glass by heating it and loosening the individual roving stands before entering into the second compounding stage. For both process, FLD were the same, indicating that while the fibre length were different, their distributions were far from monodispersed and had similar degree of polydispersity.

Table I. Number-average and weight-average fibre lengths \bar{l}_n and \bar{l}_w , and related fibre length polydispersity (FLPI) for ILC-Compression and ILC-Injection.

Sample	weight average FL (mm)	number average FL (mm)	FLD
ILC-Compression - Log	63.6	20.9	3.0
ILC-Compression - Wall	25.6	6.0	4.3
ILC-Compression - Rib	30.0	6.9	4.4
ILC-Injection - Nozzle Purge	26.7	8.9	3.0
ILC-Injection - Wall	18.1	5.9	3.0
ILC-Injection - Rib	21.9	8.6	2.6

Results in Table I further indicate that within the moulded part however the differences in FL for both moulding processes were considerably reduced, with the number-average FL being very close (within 20%) for both processes and the weight-average FL remaining higher (+40%) for ILC-Compression. Accordingly, FLD was higher for ILC-Compression (+40 to +70%). These results indicate that the moulding steps of ILC, either by compression or injection, tend to reduce the fibre lengths considerably, which results in small, yet consistent, differences in fibre length distribution from both processes. Such an observation should be reflected to some extent in the end-use properties of the moulded parts.

Mechanical Properties

Five flexural specimens taken from the mounting flange around the bottom of the parts and two flexural specimens taken from the thick wall at the center of the parts were tested (these being approximately same locations where burn off samples were taken for glass length characterization in Table I). The flexural test results are shown in Table II.

In the present study, standard deviations were generally large which should not be attributed to a lack of reproducibility in the performance from one sample to the other but to the normal envelop of properties that should be expected from specific locations within a large part.

Table II. Flexural properties of the ILC-Compression and ILC-Injection parts at two locations.

Sample Location	Flexural Modulus (GPa)		Flexural Yield Stress (MPa)		Flexural Yield Strain (%)	
	average	st. dev.	average	st. dev.	average	st. dev.
Mounting Flange (n=5)						
ILC-Compression	4650	1119	155	36	3.8	0.5
ILC-Injection	4745	1420	121	36	3.5	0.7
Thick Wall (n=2)						
ILC-Compression	4328	154	70	6	2.3	0.2
ILC-Injection	4018	1418	34	1	1.4	0.8

The flexural results in Table II indicate that for both locations the flexural moduli obtained from ILC-Compression and ILC-Injection are very close to each other and within standard deviations. These moduli are fairly low when compared to expected flexural moduli from D-LFT PP/GF properties [5], indicative of a low level of orientation of the fibres within the part. For the mounting flange specimens, the flexural strengths (yield stress) were slightly larger for the ILC-Compression (+28%), which might not be significant in light of the standard deviations obtained ($\pm 23\%$). For that specific location, flexural yield strains from both processes did not differ significantly. Both flexural strength and strain values could be considered as representative of normal D-LFT PP/GF properties.

For the thick wall specimens, the flexural modulus was slightly higher for the ILC-Compression part, which can be attributed at least partially to the higher FL reported for that location. The difference in flexural modulus could also indicate a different fibre orientation or different fibre content at this specific sampling location. As shown in Table II, higher flexural strengths and strains were also measured at this location, and more significantly, the differences between ILC-Compression and ILC-Injection were larger than in the case of the modulus. This observation reflects the known marked effect of longer fibres on strength and strain values (eventually impact too) in discontinuous fibre reinforced composite materials. While the possibility of varying fibre content or fibre orientation cannot be ruled out, it should be concluded that these flexural properties resulted at least to some extent from the longer fibres observed therein.

CONCLUSION

In conclusion having access to samples of LFT material just prior to introduction into the mould either by extruded log transfer for ILC-Compression or injection nozzle purge for ILC-Injection and the resultant moulded parts from each system has made possible for a unique study of fibre distribution, fibre length and basic mechanical properties.

For the fibre distribution pattern in the ILC-compression extrusion log, the final compounding stage in the presence of high density GF rovings resulted in the formation of an external envelope and a double helix pattern in the extruded log. Within the ILC-Injection nozzle sample, a more uniform GF structure with little GF bundling was observed. With respect to the moulded parts, the ILC-Compression reveals the presence of GF-rich zones and GF-depleted zones, indicating a somewhat uneven GF distribution within the moulded part. No specific orientation was noted, as expected from the compression of the extruded molten log. In contrast the ILC-Injection part indicates a more even distribution locally of the GF and matrix.

Fibre length results indicate that the extruded log from the ILC-Compression system contained considerably longer fibres, typically more than twice the length of the fibres in the injection nozzle purge from ILC-Injection. These results can potentially be attributed to a number of factors rooted in the different configurations of the ILC systems. However results from the moulded part show the differences in fibre length between the moulding processes were considerably reduced yet there still being a greater fibre length distribution in the ILC-Compression part. These results indicate the understanding that the moulding steps of ILC, either by compression or injection, tend to reduce the fibre lengths considerably.

Finally with respect to mechanical properties, the flexural moduli, strengths and strains obtained from ILC-Compression and ILC-Injection at several thinner wall sections (typically 3-4 mm) are very close to each other and within (or close to be within) standard deviations. For thicker wall specimens (8 mm), slightly higher flexural modulus and significantly higher flexural strengths and strains are measured for the ILC-Compression part, which can be attributed at least partially to the higher fibre lengths reported for that location. This result could also indicate a different fibre orientation or different fibre content at this specific sampling location, which could not be verified in the present study.

In summary samples from DLFT material just prior to introduction into the mould either by extruded log transfer for ILC-Compression or injection nozzle purge for ILC-Injection and the resultant moulded parts from each system clearly shows qualitative and quantitative differences.

REFERENCES

- ¹ Vaidya, U.K., Chawla, K.K. "Processing of fibre reinforced thermoplastic composites" *International Materials Reviews*, 53 (4), 2008, pp. 185-218.
- ² Krause, W., Geiger, O., Henning, F., and Eyerer, P. "Development of a technology for large scale production of continuous fiber reinforced thermoplastic composites" *Annual Technical Conference - ANTEC, Conference Proceedings*, 2005, 294-298.

³ Troester, S., Geiger, O., Henning, F., and Eyerer, P "Added value for long-fiber reinforced thermoplastic components by in-line-compounding in the LFT-DILC process" *Annual Technical Conference - ANTEC, Conference Proceedings*, 2004, 3469-3474.

⁴ Vaidya, U.K., Pillay, S. "**Cost-effective structural thermoplastic composites for automotive and transportation**" *International SAMPE Symposium and Exhibition (Proceedings)*, 52, 2007, 7 p.

⁵ **Influence of fibre length and concentration on the properties of glass fibre-reinforced polypropylene: 1. Tensile and flexural modulus**, Thomason, J.L. , M. A. Vlugs, *Composites A* 21A (1996) 417-84.